Comparative study of atmospheric and high pressure CO_2 reforming of methane over Ni/MgO-AN catalyst

Yu-He Wang and Bo-Qing Xu*

Innovative Catalysis Program, Key Lab of Organic Optoelectronics & Molecular Engineering Department of Chemistry, Tsinghua University, Beijing 100084, China

Received 6 July 2004; accepted 16 September 2004

Catalytic activity of Ni/MgO-AN prepared from alcogel derived MgO was studied for the dry reforming of methane under atmospheric as well as high pressure (1.5 MPa). Different catalytic performances are observed in the atmospheric and high-pressure reactions; while the catalyst was highly active and extremely stable under atmospheric pressure it shows a self-stabilization process under high pressure. The self-stabilization process was characterized initially by a decrease in deactivation rate with increasing the reaction time-on-stream (TOS) up to ca. 12 h and then by a thereafter stabilization during the reaction. Characterizations of the coked catalyst with TPO, TEM, SEM, TPH and XRD techniques detected very little carbon deposits (ca. 0.2 wt% of the catalyst charge) on the used catalyst under atmospheric pressure. In contrast, large amount of whisker carbon deposit (ca. 100 wt% of the catalyst charge) were formed on the used catalyst under high pressure. In the high-pressure reaction, the activity decline during the initial stage was closely related to the amount of carbon deposits on the catalyst, which also became stabilized after the catalyst had served the reaction for ca. 12 h. The carbon deposits on the used catalyst in the high-pressure reaction contained two different components (α-carbon and β-carbon) while the carbon deposits in the atmospheric pressure reaction were in the form of α-carbon. No notable sintering of metallic nickel was detected by XRD on the used catalyst in the reaction under atmospheric pressure whereas unavoidable sintering of metallic Ni particles happened within the very first hours of the high-pressure reaction.

KEY WORDS: carbon dioxide, deactivation, high pressure reforming of methane, natural gas, Ni catalyst, self-stabilization process.

1. Introduction

There has been a great interest in recent years in the more efficient use of natural gas (methane) and the reduction of greenhouse gas (i.e. CO_2) emission. The production of syngas (CO and H_2) by CO_2 reforming of methane ($CH_4 + CO_2 = 2\ H_2 + 2\ CO$) over a heterogeneous catalyst is one of the routes for the utilization methane and CO_2 resources [1–11]. The product mixture of this reaction from a stoichiometric (1:1) feed has, in comparison with steam reforming and partial oxidation, a low H_2/CO ratio (1:1) that is preferable for Fischer–Tropsch synthesis because high H_2/CO ratios favor methanation and suppress chain growth [10]. Since some reservoirs of natural gas even contain comparable concentrations of methane, the use of CO_2 provides a convenient and cheap oxygen source, for the reforming of methane [11]. Great efforts have been made on the development of highly active and stable catalysts for the CH_4/CO_2 reaction. It is well known that Ni, Ru and Rh are very effective catalyst for the CH_4/CO_2 reaction in term of CH_4 conversion and selectivity to syngas. One serious problem is carbon deposition during the reaction which deactivates the catalyst, which is most serious for the Ni catalysts. Although the noble metal catalysts (e.g. Rh and Ru) suffer from less coking, nickel catalyst is more attractive for industrial application due to its inherent availability and lower cost in comparison to the noble ones [12]. Therefore, the development of stable nickel catalysts with little or no coking is a bottleneck for the industrial application of the process. Many studies on the CH_4/CO_2 reaction under atmospheric pressure (0.1 MPa) have shown that properly nickel-magnesia catalysts have the potential of being highly resistant to coking and thus could be stable in catalyzing the reaction [13–17]. However, the problem is that the texture and physico-chemical properties of MgO can have major effects on the catalytic performance of NiO–MgO solid solution catalysts. An unsuitable MgO can lead to a low initial conversion and a long induction period [16]. In our earlier exploratory work using MgO-AN nanocrystals, which were produced by thermal processing of a $Mg(OH)_2$ alcogel in flowing nitrogen, for support of the nickel catalyst, we developed a highly active and stable Ni/Mgo-AN catalyst for the dry reforming at 0.1 MPa [17].

Generally, methane is stored and transported under high pressures, and all syntheses in GTL (syngas to liquid) process, including methanol and Fischer–Tropsch synthesis are performed under high pressures. High pressure dry reforming of methane can obtain CO-

* To whom correspondence should be addressed.
E-mail: bqxu@mail.tsinghua.edu.cn

1011-372X/05/0100–0089/0

rich syngas ($H_2/CO < 1$) from a stoichiometric (1:1) feed which can be utilized for Fischer–Tropsch, methanol and dimethyl ether synthesis. In industry, dry reforming of methane would need to be run to minimize reactor size and energy use. It would be highly desirable from an economical point of view that the CH_4/CO_2 reaction should be carried out under high pressures [18–20]. Although most research on the dry reforming of methane was carried out in atmospheric pressure, a few of studies have also appeared to explore the high pressure reforming reaction [21–34]. Tomishige *et al.* [22] investigated the effect of pressure on the dry reforming reaction over a $Ni_{0.03}Mg_{0.97}O$ solid solution catalyst that, under atmospheric pressure, is very resistant to carbon deposition. Increase in the reaction pressure was shown to induce decreased methane and CO_2 conversion rates. The product H_2/CO ratio also decreased but the rate of carbon deposition increased with significantly increasing the reaction pressure [22]. Armor and Martenak [26] also showed that an increase in the reaction pressure would accelerate carbon deposition on the Ni-based catalysts. A TiO_2-supported Ru catalyst was found stable at 2.0 MPa by Nagaoka *et al.* [29]. The catalyst showed little coking and no deactivation was observed after it was reacted for 25 h. Claridge *et al.* [30] claimed very recently that molybdenum and tungsten carbides can be stable catalyst for the high-pressure reaction; they tested the carbide catalysts for the dry reforming reaction under 0.8 MPa and detected no catalyst deactivation during 72 h.

In order to gain insight into the difference of the magnesia-supported Ni catalysts for the dry reforming of methane between atmospheric and practical high pressures, we have investigated the catalytic behavior and coking performance of the Ni/MgO-AN catalyst at 0.1 and 1.5 MPa. This paper compares the activity and stability of the catalyst under the different reaction pressures. We attempt to understand the relationship between the catalyst stability and the nature of carbon deposits on the catalyst in atmospheric and high-pressure reaction.

2. Experimental

2.1. Catalyst preparation

Magnesia support were prepared by thermal processing in flowing nitrogen of a $Mg(OH)_2$ alcogel at 923 K for 5 h. The alcogel was obtained from a $Mg(OH)_2$ hydrogel by washing with anhydrous ethanol for several times. Detailed preparation of the hydrogel was described previously in reference [17]. Following our earlier sample coding, magnesia prepared in present study was coded as MgO-AN. The average crystallite size of this MgO-AN sample was 10.1 nm. Ni/MgO-AN catalyst was prepared by wet impregnation of an aqueous solution of $Ni(NO_3)_2{\cdot}6H_2O$ into the MgO-AN nanocrystals. The loading of metallic nickel is 8.8 wt% by XRF analysis. After impregnation and drying at 393 K, the sample was calcined at 923 K for 5 h in air. The physicochemical properties of Ni/MgO-AN catalyst are listed in Table 1.

Table 1
Physico chemical properties of the Ni/MgO-AN catalyst

Catalyst	Ni loading[a] (wt%)	BET surface (m^2/g)	Reducibility (%)	Dispersion (%)
Ni/MgO-AN	8.8	48.0	23.5	14.7

[a]Detected by XRF

2.2. Activity test

The catalyst reaction was carried out with 100 mg catalyst (2∼40 mesh) in a fixed-bed quartz tubular reactor (7 mm i.d.) which was tightly fixed in a stainless steel tube. The height of the catalyst bed in the reactor was ca. 0.5 cm. A Viton O-ring pressed by a locking nut was used to prevent the gas from leaking into the ringed gap so as to eliminate the influence of the metal wall of the stainless steel tube. The reaction temperature was controlled by a thermal couple in a quartz well (6 mm o.d) that was placed down stream the reactor with its closed end inserted into the quartz wool plug supporting the catalyst bed [35]. Before the reaction, the catalyst was reduced *in situ* at 1123 K for 1 h with flowing H_2 (20 ml/min, 0.1 MPa). The flow of the reaction feed, a gas mixture of CH_4 and CO_2 ($CH_4/CO_2 = 1/1$, space velocity (GHSV) $= 1.6 \times 10^4$ ml/h·g-cat), was controlled by a mass flow controller (Brooks 5850E) and the pressure of the reaction system by a back-pressure regulate was 806, Badger Co.). The reaction products were analyzed with an on-line gas chromatograph (Varian 3400) equipped with a thermal conductivity detector. Blank test with no catalyst showed no reaction in the empty reactor.

After the catalyst had served the reaction for a specified period of time, the reaction feed was switched to inert nitrogen (high-purity), followed by cooling in nitrogen flow of the reactor to room temperature at which the used catalyst was unloaded for various characterizations.

2.3. Characterizations of catalyst

A Bruker D8 Advance X-ray Diffractometer (XRD) with Cu $K\alpha$ ($\lambda = 0.15406$ nm) was used to identify the crystal phases in the catalyst. The operation voltage was 40 kV and the current was 40 mA. The XRD patterns were recorded with a resolution of 0.02° and a scan rate of 0.3 s/point.

Carbon deposits on the used catalysts were measured by temperature programmed oxidation (TPO) in flowing air (50 ml/min) at a heating rate of 10 K/min, given in

reference [11]. A TG/DTA thermo-analyzer (Mettler-Toledo DTA/SDTA85) used for the TPO measurements.

Reactivity toward hydrogen of the carbon deposits on the used catalysts was characterized by temperature programmed hydrogenation (TPH) [11]. After reaction, the used catalyst was rapidly removed to a U-shape quartz tube (4 mm i.d.) and was then subjected to the TPH measurement up to 1173 K at heating rate of 10 K/min in pure H_2 (20 ml/min, 0.1 MPa). The CH_4 produced during the TPH measurement was monitored by an on-line mass spectrometry (Balzers MSC-200).

Transmission electron microscopy (TEM) measurements of some samples were performed on a Hitachi H-800 TEM using an accelerating voltage of 200 kV with a resolution of 1.5 nm. Scanning electron microscope (SEM) observation was carried out on the JSM 6301F using an accelerating voltage of 15 kV.

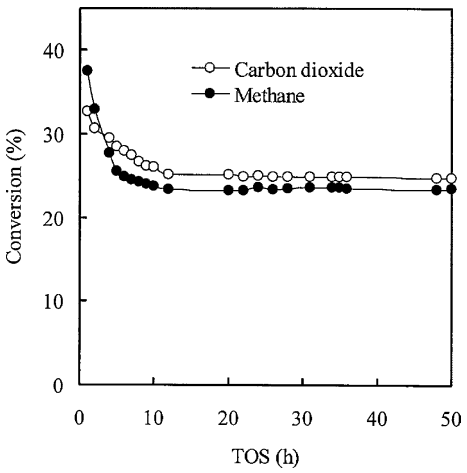

Figure 2. CH_4 (-●-) and CO_2 (-○-) conversion versus reaction time over the Ni/MgO-AN catalyst in high pressure (1.5 MPa) reaction.

3. Results

3.1. Catalytic studies

The catalytic dry reforming of methane was carried out at 1023 K over the reduced 8.8 wt% Ni/MgO-AN catalyst with a stoichiometric feed of CH_4 and CO_2 under atmospheric pressure (0.1 MPa) and high pressure (1.5 MPa). Figure 1 shows the catalytic performance of Ni/MgO-AN catalyst by conversion of methane and CO_2 in the atmospheric pressure reaction, the corresponding data in the high-pressure reaction are given in figure 2. During 50 h of reaction, the conversion of both reactants remained unchanged under atmospheric pressure (figure 1), confirming our earlier discovery that the reduced Ni/MgO-AN catalyst is highly active and stable under atmospheric pressure [17]. In contrast, the conversion of both reactant high-pressure reaction decreased with the reaction TOS up to ca. 12 h and then became stabilized at longer reaction TOS. This characteristic catalyst behavior in the high-pressure reaction can be termed as a self-stabilization of the catalyst since no external force was exerted during the reaction. Because of the unavoidable reverse water-gas shift reaction ($CO_2 + H_2 = CO + H_2O$), it can be expected that the actual conversion of CO_2 should be higher than that of CH_4 in the reaction [11,36]. Clearly, the catalytic results in figure 1 are consistent with this expectation, the conversion of methane (83.0%) being lower than that of CO_2 (86.5%). These conversions are also close the equilibrium conversion of methane (84%) and CO_2 (91%) at 1023 K under atmospheric pressure. However, in the high-pressure reaction the conversion of CH_4 (37.5%) at the very beginning of the reaction (TOS = 1 h) is higher than that of the CO_2 (32.6%) reactant. This abnormal phenomenon indicates that the conversion of CH_4 was not balanced by that of CO_2 or there was an "excessive" conversion of CH_4 at the beginning of the reaction. At TOS longer than 12 h, the conversions of CO_2 are stabilized at 23.5 and 25.0%, respectively. Since equilibrium conversions of CH_4 and CO_2 are 39.4 and 59.3% respectively, under the conditions for the high pressure reaction (CH_4/CO_2 = 1/1, 1.5 MPa and 1023 K), the stabilized reaction of CH_4 and CO_2 under the high pressure is far from its thermodynamic equilibrium.

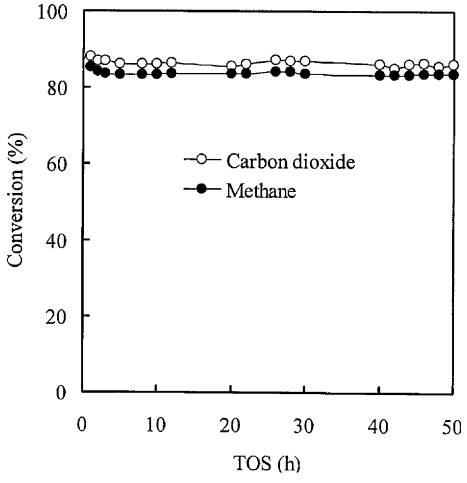

Figure 1. CH_4 (-•-) and CO2 (-o-) conversion versus reaction time over the Ni/MgO-AN catalyst in atmospheric pressure (0.1 MPa) reaction.

3.2. Characterization of catalyst

3.2.1. Amount of carbon deposits

Figure 3 compares the thermogravimetric TPO results of the Ni/MgO-AN catalyst after it was used in the reaction for 10 h under atmospheric and high pressure. No detectable weight loss was observed on the catalyst reacted in the atmospheric pressure reaction (figure 3a). In contrast, the weight loss due to carbon combustion (750–1000 K, 920 mg/g_{cat} carbon) was very distinct on the catalyst reacted in the high-pressure

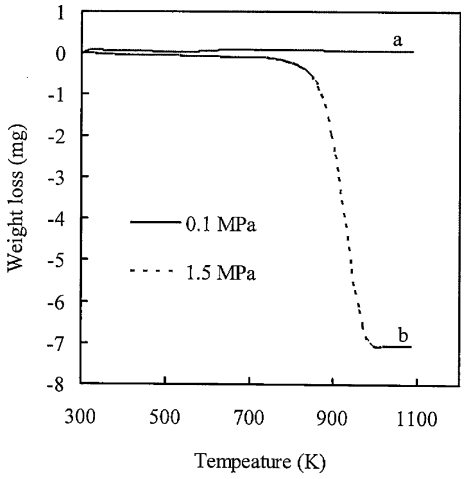

Figure 3. Thermogravimetric TPO profile of the Ni/MgO-AN catalyst after the reactions under 0.1 MPa (solid line) and 1.5 MPa (dashed line) for 10 h.

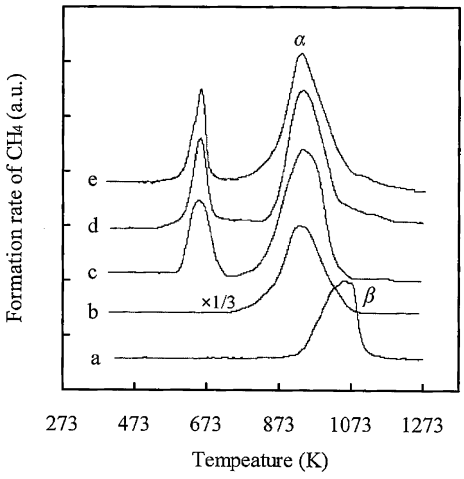

Figure 5. TPH profiles of carbon deposits on the used Ni/MgO-AN catalyst that served the CO disproportionation under 0.1 MPa for 3 h (a), CH_4 decomposition under 0.1 MPa for 3 h (b), CH_4/CO_2 reaction under 0.1 MPa for 1 h (c), 3 h (d) and 10 h (e).

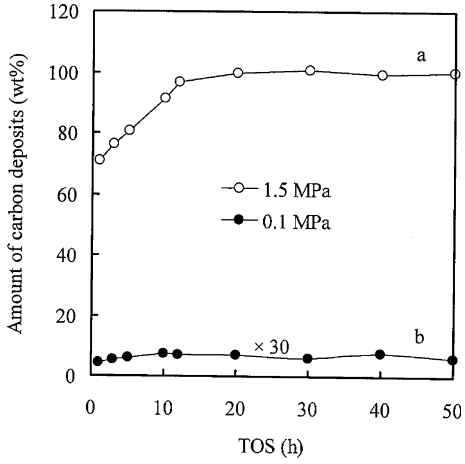

Figure 4. Effect of reaction time on the amount of carbon deposits over the Ni/MgO-AN catalyst during the reforming reaction under 0.1 MPa (-•-) and 1.5 MPa(-o-).

reaction (figure 3b). These results indicate that the reaction pressure has a remarkable effect on the carbon deposition on the Ni/MgO-AN catalyst.

Figure 4 shows the amount of carbon deposits on the used catalyst as a function of reaction time in both atmospheric and high-pressure reactions. The amount deposits in atmospheric pressure reaction is 0.2 wt% of the catalyst weight and remains unchanged during the reaction period of 50 h as shown in figure 4b. On the other hand, the amount of carbon deposits in the high-pressure reaction increased slowly with the reaction TOS from 70 wt% to a constant value of 100 wt% within 12 h (figure 4a). It is seen that within the initial 1 h of the reaction, the amount of carbon deposits could reach 70 wt% of its stabilized value. This indicates that the formation of carbon deposits was rapid at the very early period of the reaction.

3.2.2. Reactivity of carbon deposits

It has been reported that the most serious problem in CO_2 reforming of methane is the catalyst deactivation by carbon deposition via CH_4 decomposition ($CH_4 = C + 2\ H_2$) and CO disproportionation ($2\ CO = C + CO_2$) [13,22,24,28,31]. A set of experiments were designed to gain insight into the contributions of methane and CO for the carbon deposition. First, the freshly reduced Ni/MgO-AN catalyst was reacted with flowing CH_4 at 0.1 MPa and 1023 K for 3 h to collect the carbon deposits from CH_4 decomposition. The coked catalyst was then subjected to a TPH experiment to measure the reactivity of the carbon deposits. As shown in figure 5b, the TPH profile showed one methanation peak at 950 K which was designated to the hydrogenation of α-carbon. When the freshly reduced catalyst was reacted with pure CO instead of CH_4 we obtained the sample with carbon deposits from CO disproportionation. The TPH result of this sample is given as profile-a in figure 5, which reveals a methanation peak at ca. 1065 K. The related carbon deposits from CO disproportionation are designated to β-carbon. The other TPH profiles in figure 5 are featured by two peaks of methane formation with maximum temperature appearing at 660 and 950 K. These profiles are from the hydrogenation of carbon deposits on the catalysts that were related in the reaction under atmospheric pressure for 1 (figure 5c), 3 (figure 5d) and 10 h (figure 5e), respectively. The peak at 660 K can be assigned to the hydrogenation of CO_2 adsorbed on the support surface according to references [37,38]. The high temperature peak at 950 K matches well with that of α-carbon in figure 5b, indicating that the dominant carbon deposits from the methane reforming under atmospheric pressure were of the nature of α-carbon. These results suggest that any

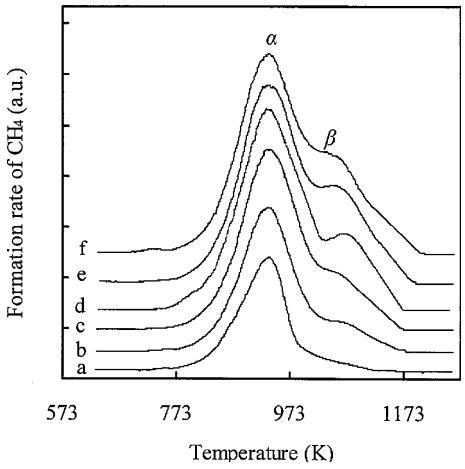

Figure 6. TPH profiles of carbon deposits on the used Ni/MgO-AN catalyst that served the CH_4/CO_2 reaction under 1.5 MPa for 1 h (a), 5 h (b), 10 (c), 12 h (d) 20 h (e) and 50 h (f).

contribution of CO disproportionation to the formation of carbon deposits on Ni/MgO-AN catalyst can be of little importance in the atmospheric pressure reaction.

Figure 6 presents the TPH profiles of carbon deposits on the catalyst that served the high-pressure reaction for 1, 5, 10. 12, 20 and 50 h, respectively. The little peak at 750 K may be due to a hydrogenation of CO_2 adsorbed on the support or carbon deposits. Compared with the low temperature peak at 660 K for the samples reacted under atmospheric pressure as shown in figure 5, the peak (750 K) was shifted to higher temperature by ca. 90 K due to the much amount of carbon deposits on used catalyst in the high-pressure reaction. In addition to the indistinct peak, two dominant peaks of methane formation were detected with maximum temperatures appearing at 950 and 1065 K, respectively. The two peaks can be assigned to the hydrogenation of α-carbon (950 K) from CH_4 decomposition and β-carbon (1065 K) from CO disproportionation according to their reactivity towards hydrogen. While the amount of both α- and β-carbon changed with increasing the reaction TOS up to 12 h, the amount of β-carbon increased apparently more rapidly than that of α-carbon. When the amounts of both kinds of carbon deposits became unchanged at TOS longer than 12 h (figure 4a), the ratio of β-carbon/(α-carbon + β-carbon) also became unchanged (figure 6e–f). This means that the amount of β-carbon increased with the reaction TOS during first 12 h of the reaction and was then kept at a constant level.

3.2.3. Morphology of catalyst surface

Figure 7 shows TEM images of the Ni/MgO-AN catalyst before (a) and after the reaction for 10 h under 0.1 (b) and 1.5 MPa (c). It can be seen that the TEM image after the reaction under atmospheric pressure is

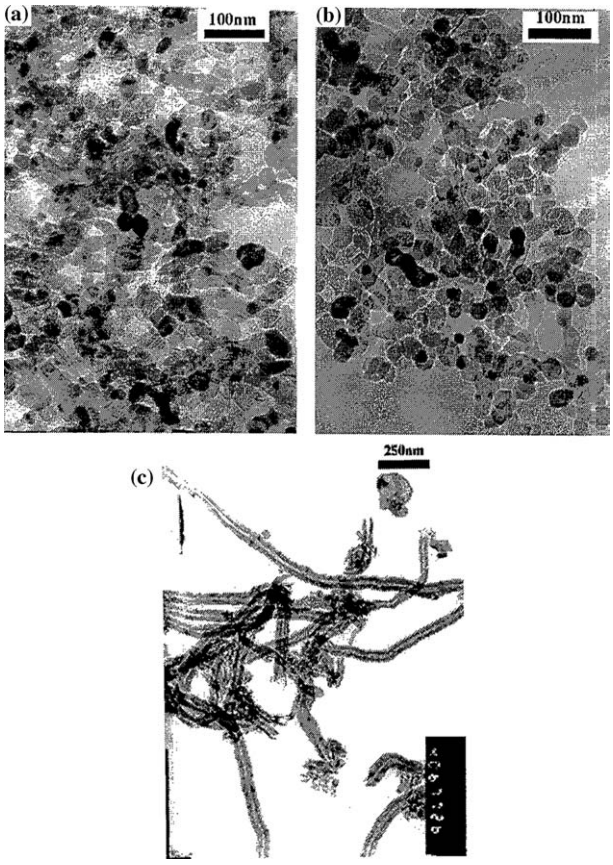

Figure 7. TEM images of the freshly reduced (a) and used (b and c) Ni/MgO-AN catalyst. The used catalyst was sampled after it had served the CH_4/CO_2 reaction under 0.1 MPa (b) and 1.5 MPa (c) for 10 h.

very similar to that of the freshly reduced catalyst which is consistent with figure 3 that no carbon deposits were formed on the catalyst figure 7b). However, a large quantity of whisker carbon (carbon nanotubes) with non-uniform diameters was observed on the used Ni/MgO-AN catalyst in the high-pressure reaction (figure 7c). The carbon nanotubes showed external-diameters of ca. 65 nm, wall thickness of ca. 25 nm and inner-diameters of ca. 15 nm. Figure 8 shows the SEM images of the whisker carbon on the used catalyst under high pressure.

3.2.4. Crystalline phases

XRD measurements give insight into the structural changes of catalyst before and the after the reactions under atmospheric and high pressure. The reduced Ni/MgO-AN shows a typical XRD pattern (figure 9a) of NiO–MgO solid solution [17]. The formation of NiO–MgO solid solution has the following consequence that only a small amount of NiO is reduced to Ni which segregates as small particles on the surface of the "solid solution" support. The absence of XRD bands due to metallic Ni on the reduced Ni/MgO-AN catalyst suggests that metallic Ni is present in the form of very small particles or coalescent Ni on NiO–MgO solid solution.

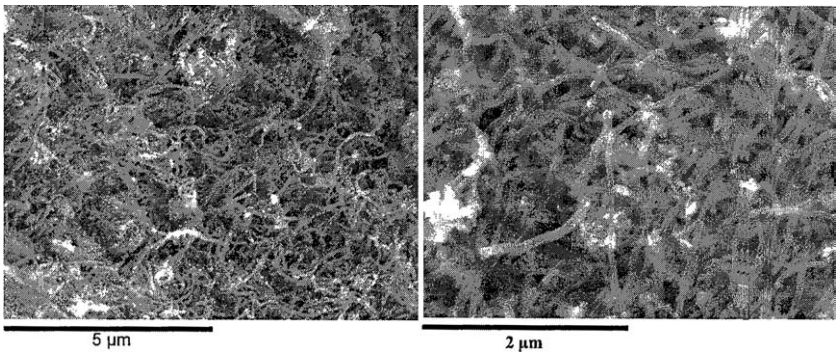

Figure 8. SEM images of the used Ni/MgO-AN catalyst that served the CH_4/CO_2 reaction under 1.5 MPa for 10 h.

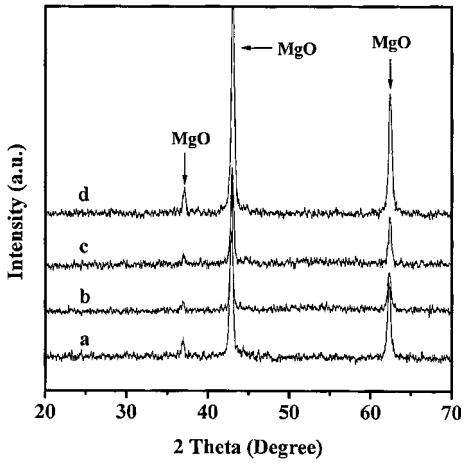

Figure 9. XRD patterns of the freshly reduced (a) and used (b–d) Ni/MgO-AN catalyst. The used catalyst was sampled after it had served the CH_4/CO_2 reaction under 0.1 MPa for 1 h (b), 3 h (c) and 10 h (d).

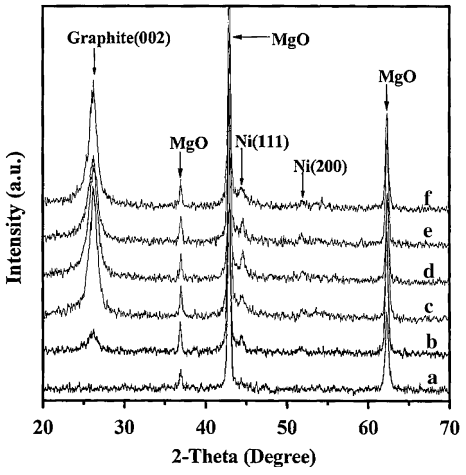

Figure 10. XRD patterns of the freshly reduced (a) and used (b–f) Ni/MgO-AN catalyst. The used catalyst was sampled after it had served the CH_4CO_2 reaction under 1.5 MPa for 1 h (b), 3 h (c), 10 h (d), 20 h (e) and 30 h (f).

Besides carbon deposits, sintering of metallic nickel may be another Cause to deactivate the catalyst in the reforming reaction [38]. The used catalyst from the atmospheric pressure reaction was characterized by XRD and the results are shown in figure 9b–d. The very similar XRD patterns indicate that the Ni particles on the used catalysts were not sintered apparently. This may be due to strong interaction between the metallic Ni and the NiO–MgO solid solution in the reduced Ni/MgO-AN catalyst [15].

Figure 10 shows the XRD patterns of the Ni/MgO-AN catalyst after it was reacted for 1, 3, 10, 20 and 30 h under 1.5 MPa. Two diffraction peaks of metallic Ni (2θ 44.5°, 51.8°) and one diffraction peak of graphite (2θ = 26.3°) were detected on the used catalyst (figure 10b–f), showing that metallic nickel particles aggregated during high-pressure reaction. It should be mentioned that intensity for the metallic Ni on the used catalysts was independent of the reaction TOS in figure 10, which suggests that the sintering or aggregation of metallic nickel occurred only at the very beginning of the high-pressure reaction.

4. Discussion

Among the factors leading to catalyst deactivation in CO_2 reforming of methane, carbon deposition is the most serious problem [14,38]. Thermodynamic calculations showed that the potential for carbon formation in the reaction is high at a feed CO_2/CH_4 ratio of 1.0 or less [16]. However, the Ni/MgO-AN catalyst remained stable the without detectable deactivation for up to 50 h on stream in the atmospheric pressure reaction. This indicates that the formation process of carbon deposits is controlled by the reaction kinetics over the Ni/MgO-AN catalyst. The formation of NiO–MgO solid solution in the reduced Ni/MgO-AN catalyst has important implications:high dispersion or small particle size of the reduced metallic Ni, strong basicity of the support surface and favorable nickel-support interactions [16]. The basicity and the strong metal-support interaction in NiO–MgO solid solution catalyst, which inhibit carbon deposition and sintering of the Ni particles, are responsible for the high activity and stability of the catalyst for the CO_2 reforming of CH_4 under atmo-

spheric pressure. One of the factors that inhibit carbon deposition is the strong Lewis basicity of MgO, which causes strong chemisorption of CO_2 and leads to a high concentration of CO_2 at the catalyst surface, which can accelerate the reaction of CO_2 with the reactive carbonaceous intermediates to form CO, resulting in the reduction of coke formation. On the other hand, a high concentration of adsorbed CO_2 can also inhibit the disproportionation reaction of CO since CO_2 is a product of CO disproportionation. Therefore, the very small and seemingly unchanged amount (0.2 wt%) of carbon deposits in the atmospheric pressure reaction can be explained by a balanced deposition and volatilization of carbon on the working catalyst during the reaction. In addition, the control of Ni particle sizes via solid solution formation in the present Ni/MgO-AN catalyst may also play an important role in inhibiting the carbon deposition and in preventing sintering of the metallic Ni. This occurs because the formation of the solid solution could ensure cluster sizes of the metallic Ni below the Ni ensemble size needed for carbon deposition from CH_4 decomposition and CO disproportionation [16].

No formation of large Ni particles in our XRD data of the used catalysts (figure 9) provides a piece of strong evidence for the high resistance to sintering of the metal component in the atmospheric pressure reaction. Such high resistance of the Ni particles can be associated with the strong interaction between the metallic Ni and NiO–MgO solid solution in the Ni/MgO-AN catalyst [39]. Thus, it seems that the long-term stability of the Ni/MgO-AN catalyst in the atmospheric pressure reaction is related to its capability of maintaining a well-balanced deposition and elimination of coke at the surface as well as a strong resistance of the small Ni particles to sintering under the working conditions [40,41].

It is interesting to recall that the carbon deposits produced in the atmospheric pressure reaction are composed of only the α-carbon from CH_4 decomposition; β-carbon from CO disproportionation was not present (figure 5). According to Swaan *et al*. [42], among the two forms of carbon deposits, only the stable form arising possibly from the CO disproportionation would poison the Ni catalyst, and the other less stable form arising from methane activation would be rapidly accumulated on the catalyst poisoning the catalysts to a much less extent. Thus, the high activity and stability of the Ni/MgO-AN catalyst in the atmospheric pressure reaction can be mainly due to an efficient inhibition of the CO disproportionation reaction on the working catalyst. In addition to prevent the sintering of small Ni particles, the strong metal-support interaction induced by the formation of NiO–MgO solid solution in the Ni/MgO-AN catalyst would reduce the electron-donor ability of metallic Ni in the activation of CO molecules [43], leading to efficient inhibition of the disproportionation reaction of CO.

When the reaction was carried out under the high pressure, the catalytic performance of the same Ni/MgO-AN catalyst was quite different from it was under the atmospheric pressure. The highly active and stable catalysis of the catalyst in the reaction under atmospheric pressure (figure 1) was not maintained but replaced by the self-stabilization catalysis under the high pressure (figure 2). Consequently, significant sintering of Ni particles on the used catalyst under the high pressure was detected by the XRD measurements shown in figure 10. Also, the amount of carbon deposits was seen to increase with the reaction TOS of the high-pressure reaction (figures 4a and 10). These observations demonstrate that the strong interaction between the Ni particles and the solid solution support is not sufficient in preventing the sintering and deactivation of the freshly reduced catalyst in the high-pressure reaction.

It is believed that strong metal-support interaction would inhibit the formation of large metal clusters needed for coke deposition [16,44]. Thereby, the sintering of Ni particles in the early stage of the high-pressure reaction would result in an increase in the rate of carbon deposition on the working catalyst. Fortunately, the formation of carbon deposits did not continue after 12 h in the high-pressure reaction, enabling the self-stabilization catalysis. The catalyst self-stabilization after the deactivation seems to suggest that the catalyst may have two groups of active sites for the reaction under the high pressure. Actually, two groups of metallic Ni sites were found in the reduced Ni/MgO-AN catalyst according to our earlier H_2-TPD measurement of the catalyst [45]. It can be deduced that the two groups of active sites functioned differently in the high-pressure reaction. Ito *et al*. [46] suggested that the metallic sites in interaction with the support participated in the reforming reaction while those had no interaction with the support were responsible for the carbon deposition. When the sites responsible for the carbon deposition become blocked in the high-pressure reaction, the formation of carbon deposits would stop to increase with the reaction TOS. Subsequently, the other group of the metallic sites would function to give a stable activity for the reaction figure 2).

Since CO disproportionation and formation of β-carbon usually occur on larger ensembles of the metallic Ni, the sintering of Ni particles in the high-pressure reaction would promote the accumulation of β-carbon. The thermodynamics of the disproportionation reaction ($2\ CO = C + CO_2$) is another driving force for the formation of β-carbon under atmospheric pressure. Thereby, the sintering of metallic Ni at the beginning of the high-pressure reaction was accompanied by the formation of β-carbon. Because the rate of carbon deposition from CO disproportionation is slower than that from CH_4 decomposition [38], the α-carbon was present as the dominant form of the carbon deposits at the early stage of the high-pressure reaction. Thus, the

"excessive" conversion of CH_4 at the beginning of the reaction (figure 2) can be explained by a rapid formation of the carbon deposits from CH_4 decomposition. Despite that the formation of β-carbon was subordinate at the early stage of the reaction, the fraction of β-carbon in the carbon deposits continued to increase significantly with the reaction TOS up to ca. 12 h when the catalyst became self-stabilized under the high pressure (figure 2). Thus, the coincident behavior of the catalyst self-stabilization and the accumulation of β-carbon could imply that the catalyst deactivation in the early period of the high-pressure reaction is mainly associated with the accumulation of β-carbon on the catalyst surface.

5. Conclusions

The present data show that Ni/MgO-AN catalyst exhibited different catalytic activity and stability in the atmospheric and high-pressure reactions for the dry reforming of methane; while the catalyst was highly active and stable under atmospheric pressure it developed a self-stabilization process during the reaction under high pressure.

The carbon deposits formed on the stable catalyst in the reaction under atmospheric pressure were little (0.2%) and can be assigned to the α-carbon from CH_4 decomposition. In contrast, the carbon deposits on the catalyst in the high-pressure reaction contained the α-carbon from CH_4 decomposition as well β-carbon from CO disproportionation. The solid solution NiO–MgO in the NiO/MgO-AN catalyst, which can inhibit the formation of carbon deposits in the atmospheric pressure reaction, becomes unable to inhibit the formation of carbon deposits in the high-pressure reaction. In the high-pressure reaction, accumulation of β-carbon on the working catalyst may be responsible for the activity decline of the catalyst during the self-stabilization process.

Acknowledgments

The authors thank the Natural Science Foundation (NSF) of China (grant: 20125310) and the National Basic Research Program of China (grant: 2003CB615804) for financial support of this work.

References

[1] A.T. Ashcroft, A.K. Cheetham, M.L.H. Green and P.D.F. Vernon, Nature 352 (1991) 225.
[2] Z.L. Zhang and X.E. Verykios, Catal. Today 21 (1994) 589.
[3] S.B. Wang and G.Q. Lu, Energy Fuels 12 (1998) 248.
[4] J.M. Wei, B.Q. Xu, J.L. Li, Z.X. Cheng and Q.M. Zhu, Appl. Catal. A 196 (2000) L167.
[5] S.H. Seok, S.H. Choi, E.D. Park, S.H. Han and J.S. Lee, J. Catal. 209 (2002) 6.
[6] J.A.C. Dias and J.M. Assaf, Catal. Today 85 (2003) 59.
[7] S. Menad, P.F. Aparicio, O. Cheri, A.G. Ruiz and I. Rodriguez-Ramos, Catal. Lett. 89 (2003) 63.
[8] Z.W. Liu, H.S. Roh and K.W. Jun, J. Ind. Eng. Chem. 9 (2003) 267.
[9] K. Asami, X.H. Li, K. Fujimoto, Y. Koyama, A. Sakurama, N. Kometani and Y. Yonezawa, Catal. Today 84 (2003) 27.
[10] M.C.J. Bradford and M.A. Vannice, Appl. Catal. A 142 (1996) 73.
[11] B.Q. Xu, J.M. Wei, Y.T. Yu, J.L. Li and Q.M. Zhu, Topics Catal. 22 (2003) 77.
[12] Z.P. Hao, H.Y. Zhu and G.Q. Lu, Appl. Catal. A 242 (2003) 275.
[13] K. Tomishge, O. Yamazaki, Y.G. Chen, K. Yokoyama, X.H. Li and K. Fujimoto, Catal. Today 45 (1998) 35.
[14] Y.G. Chen, K. Tomishige, K. Yokoyama and K. Fujimoto, J. Catal. 184 (1999) 479.
[15] E. Ruckenstein and Y.H. Hu, Appl. Catal. A 133 (1995) 149.
[16] E. Ruckenstein and Y.H. Hu, Appl. Catal. A 133 (1995) 149.
[17] B.Q. Xu, J.M. Wei, H.Y. Wang, K.Q. Sun and Q.M. Zhu, Catal. Today 68 (2001) 217.
[18] K. Tomishige, Y. Matsuo, Y. Yoshinaga, Y. Sekine, M. Asadullah and K. Fujimoto, Appl. Catal. A 223 (2002) 225.
[19] N. Armor, Res. Chem. Intermed. 24 (1998) 105.
[20] T.S. Christensen and I.L. Primdahl, Hydrocarbon Process 73 (1994) 39.
[21] K. Nagaoka, K. Takanabe and K. Aika, Chem. Commun. (2002) 1006.
[22] K. Tomishige, Y. Himeno, Y. Matsuo, Y. Yoshinaga and K. Fujimoto, Ind. Eng. Chem. Res. 39 (2000) 1891.
[23] K. Nagaoka, K. Takanabe and K. Aika, Appl. Catal. A 255 (2003) 13.
[24] D. Chen, R. Lødeng, A. Anundskås, O. Olsvik and A. Holmen, Chem. Eng. Sci. 56 (2001) 1371.
[25] A.J. Brungs, A.P.E. York, J.B. Claridge, C. Marquez-Alvarez and M.L.H. Green, Catal. Lett. 70 (2000) 117.
[26] J.N. Armor and D.J. Martenak, Appl. Catal. A206 (2001) 231.
[27] W. Pan and C.S. Song, Abstracts of Papers of the Am. Chem. Soc., 219 71-Petr Part 2 Mar 26 2000.
[28] K. Nagaoka, M. Okamura and K. Aika, Catal. Commun. 2 (2001) 255.
[29] K. Nagaoka, K. Takanabe and K. Aika, Appl. Catal. A 255 (2003) 13.
[30] J.B. Claridge, A.P.E. York, A.J. Brungs, C. Marquez-Alvarez, J. Sloan, S.C. Tsang and M.L.H. Green, J. Catal. 180 (1998) 85.
[31] A. Shamsi and C.D. Johnson, Catal. Today 84 (2003) 17.
[32] Y. Matsuo, Y. Yoshinaga, Y. Sekine, K. Tomishige and K. Fujimoto, Catal. Today 63 (2000) 439.
[33] K. Tomishige, Y. Matsuo, Y. Sekine and K. Fujimoto, Catal. Commun. 1 (2001) 11.
[34] F.B. Noronhaa, A Shamsib, C. Taylorb, E.C. Fendleyc, S. Stagg-Williamsc and D.E. Resascoc, Catal. Lett. 90 (2003) 13.
[35] Q.J. Zhang, D.H. He, J.L. Li, B.Q. XU, Y. Liang and Q.M. Zhu, Catal. Appl. A 224 (2002) 201.
[36] B.Q. Xu, J.M. Wei, Y.T. Yu, Y. Li, J.L. Li and Q.M. Zhu, J. Phys. Chem. B107 (2003) 5203.
[37] Y.G. Chen, K. Tmmishige and K. Fujimoto, Appl. Catal. A 161 (1997) L11.
[38] K. Tomishige, Y.G. Chen and K. Fujimoto, J. Catal. 181 (1999) 91.
[39] Y.H. Hu and E. Ruckenstein, Catal. Lett. 43 (1997) 71.
[40] Z.L. Zhang, V.A. Tsipouriari, A.M. Efstathiou and X.E. Verykios, J. Catal. 158 (1996) 51.
[41] S.B. Wang and G.Q.M. Lu, Appl. Catal. B 16 (1998) 269.
[42] H.M. Swaan, V.C.H. Koll, G.A. Martin and C. Mirodatos, Catal. Today 21 (1994) 571.
[43] Y.H. Hu and E. Ruckenstein, Catal. Lett. 36 (1996) 145.
[44] J.R. Rostrup-Nielsen, J. Catal. 85 (1984) 31.
[45] Y.H. Wang, H. Wang, Y. Li, Q.M. Zhu and B.Q. XU, *Topics Catal.*, (in press).
[46] M. Ito, T. Tagawa and S. Goto, Appl. Catal. A 177 (1999) 15.